

Building Real-time Awareness of Out-of-distribution in Trajectory Prediction for Autonomous Vehicles

Tongfei (Felicia) Guo¹, Taposh Banerjee², Rui Liu³, and Lili Su¹ 

Abstract

Trajectory prediction describes the motions of surrounding moving obstacles for an autonomous vehicle; it plays a crucial role in enabling timely decision-making, such as collision avoidance and trajectory replanning. Accurate trajectory planning is the key to reliable vehicle deployments in open-world environment, where unstructured obstacles bring in uncertainties that are impossible to fully capture by training data. For traditional machine learning tasks, such uncertainties are often addressed reasonably well via methods such as continual learning. On the one hand, naively applying those methods to trajectory prediction can result in continuous data collection and frequent model updates, which can be resource-intensive. On the other hand, the predicted trajectories can be far away from the true trajectories, leading to unsafe decision-making. In this paper, we aim to establish real-time awareness of out-of-distribution in trajectory prediction for autonomous vehicles. We focus on the challenging and practically relevant setting where the out-of-distribution is deceptive – that is, the one not easily detectable by human intuition. Drawing on the well-established techniques of sequential analysis, we build real-time awareness of out-of-distribution by monitoring prediction errors using the quickest change point detection (QCD). Our solutions are lightweight and can handle the occurrence of out-of-distribution at any time during trajectory prediction inference. Experimental results on multiple real-world datasets using a benchmark trajectory prediction model demonstrate the effectiveness of our methods.

1 INTRODUCTION

Autonomous vehicles (AVs) have been transforming transportation systems. Google Waymo rides surging in San Francisco and Baidu Apollo’s robotaxis comprising 3% of Wuhan’s taxi fleet shows the rapidly increasing adoption of autonomous transport [1, 2]. Besides, it is estimated that 40% of vehicles will be autonomous by 2040 [3]. Towards widespread deployment, autonomous vehicles must operate reliably in open-world environments, which inherently harbor uncertainty that stems from factors such as unfamiliar traffic scenes and unforeseeable distributional shifts.

Accurate trajectory prediction of surrounding moving objects is a key enabler of timely and informed decision-making, which is crucial for safe driving [4]. Trajectory prediction for autonomous vehicles has received intensive research attention with a recent focus on designing advanced deep neural networks [5, 6, 7, 8, 9]. In addition, various uncertainty awareness and uncertainty quantification methods have been developed [10, 11, 12, 13], considering both aleatoric uncertainty

^{*1}Tongfei (Felicia) Guo and Lili Su are with the Electrical and Computer Engineering Department, Northeastern University, Boston, USA. Email: {guo.t, l.su}@northeastern.edu

^{†2}Taposh Banerjee is with the Industrial Engineering Department, University of Pittsburgh, Pittsburgh, USA. Email: taposh.banerjee@pitt.edu

^{‡3}Rui Liu is with the College of Aeronautics and Engineering, Kent State University, Kent, USA. Email: rliu11@kent.edu

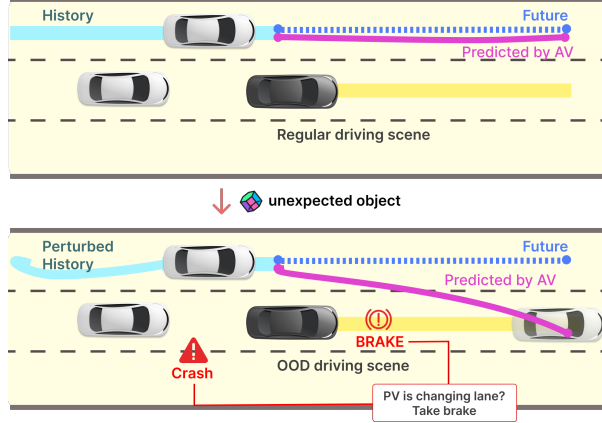


Figure 1: Comparison of an in-distribution scene with an out-of-distribution (OOD) scene. In the OOD scenario, an unexpected object (e.g. construction debris, the part of the car that the front car fell off), is left over on the road, which force the target vehicle deviates slightly from its usual path. Then, the ego vehicle may mispredict a lane change and abruptly brake, risking a rear-end collision.

(originating from inherent data noise) and epistemic uncertainty (arising from model limitations). Though with more complex neural networks and with a larger volume of training datasets, epistemic and aleatoric uncertainties can be mitigated to some extent, a trajectory prediction model still suffers significant performance degradation when entering out-of-distribution (OOD) scenarios (Fig. 1) [14, 15, 16, 17]. In this paper, we focus on the challenging and practically relevant setting where the OOD is deceptive – that is, the involved out-of-distribution is not easily detectable by human intuition.

For traditional machine learning tasks, the issues of distributional shifts and unseen data often can be addressed reasonably well via methods such as continual learning [18, 19]. Unfortunately, naively applying those methods to trajectory prediction can result in continuous data collection and frequent model updates, which can be resource-intensive. In addition, it could introduce frequent interruptions due to unnecessary model updates and end up with significant resource waste when OOD scenarios occur sparsely.

OOD detection has emerged as a popular area in machine learning [20, 21, 22, 23]. Existing methods have several limitations when applied to trajectory prediction. First, real-world driving scenarios often involve complex and temporally correlated disturbances that are harder to detect [24, 23]. Second, existing OOD detection approaches use individual anomaly scores at each timestep rather than considering the full history of anomaly scores, overlooking potential improvements offered by sequential hypothesis testing [25]. Quickest change-point detection (QCD) methods have the potential in overcoming these limitations by focusing on identifying shifts in the underlying data distribution over time [26, 27, 28, 29]. QCD algorithms are optimized to detect the change in distribution with the formally guaranteed minimum possible delay, subject to a constraint on the tolerable rate of false alarms.

Contributions. Drawing on the well-established techniques of sequential analysis, we build real-time awareness of out-of-distribution by monitoring prediction errors using QCD. The main contributions of this work are as follows:

1. We are the first to apply QCD methods to detect OOD on multiple real-world trajectory prediction datasets. Our solutions are lightweight (monitoring a scalar variable of the prediction errors only) and can handle the occurrence of OOD at any time during inference.
2. To capture deceptive OOD in our experiments, we use the adversarial trajectory perturbation

designed in [17] to generate out-of-distribution trajectories.

3. Experimental results on multiple real-world datasets using a benchmark trajectory prediction model demonstrate the effectiveness of our methods.

2 Related Work

2.1 Trajectory Prediction

Classical trajectory prediction approaches for autonomous vehicles include Monte Carlo Simulation [30, 31], Bayesian networks [32, 33], Hidden Markov Models (HMM) [34, 35] etc. More advanced approaches primarily fall into two categories: Recurrent Neural Network (RNN)-based methods and probabilistic modeling [36, 37, 38, 39, 40, 41, 42, 43]. RNN-based approaches, particularly those employing Long Short-Term Memory (LSTM) networks, are widely used to generate smooth and continuous vehicle trajectories. For instance, [37, 38] predict both longitudinal and lateral trajectories of vehicles by training on a large dataset that covers diverse traffic conditions. [39, 40, 41] study vehicle maneuver prediction by learning a probabilistic model that assigns likelihoods to different driving maneuvers. Probabilistic models have also been utilized to address lane-change behaviors [42, 43], where the model considers potential collisions with nearby vehicles to minimize false alarms. In addition, hybrid approaches that integrate physics-based and maneuver-based methods to account for short-term and long-term effects are considered in [44, 45].

2.2 Uncertainty Quantification and Awareness

Existing methods for handling prediction uncertainty typically use different network architectures and uncertainty estimation techniques, or are tested on various datasets with a wide range of evaluation metrics. Common approaches for quantifying aleatoric uncertainty include Maximum Likelihood Estimation (e.g., Direct Modeling) [46, 47]. For estimating epistemic uncertainty, popular methods include Monte Carlo dropout [48] and deep ensembles [49]. However, these uncertainty estimating techniques require significant computational resources, introduce additional latency, and have a larger memory footprint. They may pose considerable challenges in safety-critical applications (i.e., decision-making systems of AVs) with stringent time constraints and limited computational capacity.

2.3 Out-of-distribution (OOD) Detection

Hendricks et al. [20] pioneer the first approach for OOD detection, showing that a softmax classifier can effectively distinguish between in-distribution and OOD samples. Lee et al. [21] use generative adversarial networks (GANs) to generate synthetic OOD examples, minimizing Kullback–Leibler (KL) divergence to enhance classifier confidence. Later, [22] apply Mahalanobis distance in feature space to measure OOD probability density, enhancing performance with ensemble techniques and logistic regression-based detection.

As a method that can provide formal performance guarantees in detecting distributional changes, QCD algorithms are widely applied in many domains such as healthcare [50, 51, 52, 53], climate change [54, 55, 56], speech recognition [57, 58], image analysis [59], and cyber security [60, 61, 62]. In classic formulation of QCD problem, a sequence of observations undergoes an abrupt shift in its distribution at an unknown point in time. The objective is to detect this change as quickly as possible while controlling for false alarms [63, 64, 65, 66, 67]. The cumulative sum (CUSUM) statistic

remains a widely used method for detecting change points due to its simplicity and computational efficiency [68, 26], and it is optimal in minimizing detection delays for a given false alarm rate [64].

3 Problem Formulation

3.1 Trajectory Representation and Prediction Framework

Let the state of an object i (e.g., a vehicle or a pedestrian) at time t be denoted by s_t^i , which includes spatial coordinates and possibly other features. The trajectory of object i over a time range from t_1 to t_2 is represented as a sequence of states $s_{t_1:t_2}^i = \{s_{t_1}^i, \dots, s_{t_2}^i\}$. At each time frame, a trajectory prediction model uses the historical trajectories of surrounding objects to forecast their future trajectories. The predictions are optimized to follow a distribution similar to the ground-truth future trajectories.

At any given time t , let N represent the number of observed objects. We denote the number of time frames in history as L_I and in the future as L_O . The history trajectories at time t are represented by $H_t = \{H_t^i = s_{t-L_I+1:t}^i \mid i \in [1, N]\}$, the ground-truth future trajectories are $F_t = \{F_t^i = s_{t+1:t+L_O}^i \mid i \in [1, N]\}$, and the predicted future trajectories are $P_t = \{P_t^i = p_{t+1:t+L_O}^i \mid i \in [1, N]\}$, where p_t^i is the predicted state of object i at time t .

Metrics

For a fair comparison, we employ the metrics *Average displacement error* (ADE) and *Final displacement error* (FDE) [69] from the ICRA 2020 *nuScenes* prediction challenge. ADE and FDE are defined as follows: Let n be the target vehicle, which can be arbitrarily chosen.

$$\begin{aligned} \text{ADE}_t &= \frac{1}{L_O} \sum_{r=1}^{L_O} \|p_{t+r}^n - s_{t+r}^n\| \\ \text{FDE}_t &= \|p_{t+L_O}^n - s_{t+L_O}^n\|. \end{aligned}$$

While ADE averages the error over the prediction horizon, and FDE measures the error at the final time step, we also include *Root Mean Squared Error* (RMSE) that measures the square root of the average squared differences between predicted and actual values, calculated as:

$$\text{RMSE}_t = \sqrt{\frac{1}{L_O} \sum_{r=1}^{L_O} \|p_{t+r}^n - s_{t+r}^n\|^2}$$

3.2 Entering Out-of-distribution from In-distribution

Let the ego autonomous vehicle be equipped with a given trajectory prediction model of surrounding vehicles, denoted by NN, and operate on the road. A driving route consists of many different scenes, such as driving along the highway at the very beginning, then exiting the highway, and entering a busy traffic crossing. It may happen that the ego vehicle encounters an out-of-distribution scene starting from the route source or that the ego vehicle enters into an out-of-distribution scene from in-distribution scenes at some unknown time γ .

Our goal is to enable the ego vehicle to quickly be aware of entering an out-of-distribution even when the out-of-distribution can arise at any time. Intuitively, the prediction error patterns of NN on in-distribution scenes and on out-of-distribution scenes are

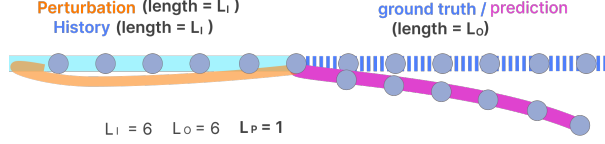


Figure 2: An example of a deceptive OOD scene occurs when the target vehicle follows a slightly deviated trajectory from an in-distribution path. The ego vehicle may incorrectly predict a lane change and react by suddenly braking, potentially causing a rear-end collision.

different. Otherwise, the given NN performs exactly the same, i.e., no performance degradation. Observing this, we draw tools from sequential analysis to monitor the error patterns (ADE, FDE, and RMSE, respectively) of the trajectory prediction model NN. Let x_t denote the error at time t .

3.3 OOD Scene Generation

We focus on building awareness of deceptive OOD driving scenes. In our experiments, we generate such scenes through small, calibrated perturbations to the in-distribution of the target vehicle’s historical trajectories following the adversarial trajectory construction in [17]. Let NN be a given deep network trajectory prediction model. Considering the perturbation Δ , the target vehicle’s past trajectory H^n , and the constraint function C , we determine the largest coefficient θ (with $0 \leq \theta \leq 1$) that scales the perturbation to $\theta\Delta$ while ensuring it adheres to all constraints. Let $\Delta = \{\Delta_1, \dots, \Delta_{L_I}\} \in \mathbb{R}^{2 \times L_I}$. The perturbation is applied to the historical trajectory over a length of L_I by solving the following optimization problem

$$\max_{\Delta} C(\Delta, \text{NN}, \{H_t^n\}_{t=L_I}^{L_I}, f), \quad (1)$$

where

$$C(\Delta, \text{NN}, \{H_t^n\}_{t=L_I}^{L_I}, f) = \sum_{t=L_I}^{L_I} f(P_t^n, F_t^n)$$

is the prediction error, $P_t^n = \text{NN}(H_t^n + \Delta_{t-L_I+1:t})$ is the predicted trajectory on the perturbed history trajectory, $f \in \{\text{ADE}, \text{FDE}, \text{RMSE}\}$ denotes the chosen metrics. In addition, hard constraints are considered when making perturbation such as bounds of physical properties and deviation [17].

4 Methods

In this section, we present the key methods used for detecting OOD events, focusing on CUSUM as the primary algorithm, with Z-Score and Chi-Square tests serving as benchmark comparisons. CUSUM is a mature method known for its robust theoretical foundation and ability to quickly and reliably detect distributional shifts [70, 71, 72]. In particular, CUSUM is designed to minimize detection delay while keeping the false alarm rate within acceptable bounds, providing formal performance guarantees in dynamic environments. As benchmarks, the Z-Score and Chi-Square methods are commonly used in literature for comparison [73, 74, 75, 76].

4.1 CUSUM Change-point Detection

In scenarios like safe driving under OOD conditions, prediction error patterns can shift unpredictably. CUSUM addresses this by monitoring cumulative deviations in the log-likelihood ratio

Algorithm 1: CUSUM with Parameterized Models

Input: Threshold $b > 0$

Output: Change point τ if detected

```
1 Initialize  $W_0 \leftarrow 0$ ;  
2 Learn parameters  $\phi$  and  $\theta$  from the data ;  
3  $f_\phi(x_t)$  /* pre-change distribution */  
4  $g_\theta(x_t)$  /* post-change distribution */  
5 while true do  
6   Receive new data point  $x_t$ ;  
   /* Compute the log-likelihood ratio */  
7    $\text{LLR}(x_t) = \log \frac{g_\theta(x_t)}{f_\phi(x_t)}$   
8    $W_{t+1} \leftarrow \max(W_t + \text{LLR}(x_t), 0)$ ;  
9   if  $W_{t+1} \geq b$  then  
10    Declare the detection of a change point;  
11    Break;  
12  end  
13 end
```

between expected and observed distributions. The method uses the following key equation:

$$\tau = \inf\{t \geq 1 : W_t \geq b\},$$

where

$$W_t = \begin{cases} \max\{W_{t-1} + \log L(x_t), 0\}, & \text{for } t \geq 1; \\ 0, & \text{for } t = 0, \end{cases}$$

and $L(x_t) = \frac{g_\theta(x_t)}{f_\phi(x_t)}$ is the likelihood ratio. For ease of exposition, we assume that f and g are parameterized families of distributions f_ϕ and g_θ , for example, Gaussian or Gaussian mixture distributions. If the distributions are Gaussian, then the parameters ϕ and θ contain information on the means and variances of these distribution families. These parameters are learned from training data.

Recall that $\{x_t\}$ is a sequence of random variables in which we wish to detect a change in distribution from f to g . The CUSUM algorithm is based on the following intuition: After a change-point γ , the observations x_t are distributed according to g_θ , and the expected log-likelihood ratio $\mathbb{E}_{t \geq \gamma}[\log(\frac{g_\theta(x_t)}{f_\phi(x_t)})]$ equals the Kullback-Leibler divergence $\text{DKL}(g_\theta \parallel f_\phi)$, which is positive. Conversely, before γ , the observations are governed by f , and $\mathbb{E}_{t < \gamma}[\log(\frac{g_\theta(x_t)}{f_\phi(x_t)})] = -\text{DKL}(f_\phi \parallel g_\theta)$, which is negative. Consequently, with an increasing number of observations, the cumulative sum $\sum_{t:t \geq \gamma} \log(\frac{g_\theta(x_t)}{f_\phi(x_t)})$ is expected to exceed the threshold b . The $\max\{\cdot, 0\}$ function in the statistic W_t reduces the impact of random fluctuations in the log-likelihood ratio and helps identify the change-point γ . The threshold b controls the sensitivity of the detection; increasing b makes the algorithm less prone to false alarms but also delays the detection of actual changes.

4.2 Z-Score Time-series Detection

The Z-Score method detects change points by measuring how much a data point deviates from a moving average. For each time point t , the Z-Score method calculates the moving average μ_t over a defined window size w , as: $\mu_t = \frac{1}{w} \sum_{i=t-w+1}^t x_i$, where x_i represents the time points. Next, the

moving standard deviation σ_t is computed as: $\sigma_t = \sqrt{\frac{1}{w} \sum_{i=t-w+1}^t (x_i - \mu_t)^2}$. Using these, the Z score z_t for each data point x_t at time t is then calculated as: $z_t = \frac{x_t - \mu_t}{\sigma_t}$

A threshold is set for the Z-Score, often based on how sensitive the detection should be. When the absolute value of the Z-Score $|z_t|$ exceeds the threshold, it indicates that the data point x_t is significantly deviating from the moving average. This signals a potential change point:

$$\tau_s = \min\{t : |z_t| > \text{threshold}\}$$

In summary, the Z-Score method detects change points by identifying data points whose deviations (in terms of θ , variation, and standard deviation) exceed a pre-set threshold, indicating a shift in the underlying distribution.

4.3 Chi-Square Time-series Detection

Chi-Square test commonly used to evaluate the independence of categorical variables and the fit between observed and expected frequencies. Specifically, we use Pearson’s chi-square test to compare observed frequencies in the time-series with expected frequencies under normal behavior [77]. Significant deviations from the expected values suggest potential anomalies. The test statistic is computed as follows:

$$\chi^2 = \sum \frac{(O_i - E_i)^2}{E_i}$$

where O_i and E_i represent observed and expected frequencies, respectively. The null hypothesis assumes that no significant difference exists between these frequencies, and any large chi-square value would indicate an anomaly.

5 Experiments and Results

Datasets. Table 1 summarizes the characteristics of the three datasets used. Apolloscape [78] the dataset consists of camera-based images, LiDAR- scanned point clouds, and about 50min manually annotated trajectories captured at 2 frames per second. NGSIM [79] dataset consists of trajectories of the freeway (US-101 and I-80) traffic sampled at a frequency of 10 Hz over 45 minutes. NuScenes [80] dataset collected 1000 driving scenes in Boston and Singapore, two cities that are known for their dense traffic and highly challenging driving situations. The scenes of 20- second length are manually selected to show a diverse and interesting set of driving maneuvers, traffic situations, and unexpected behaviors. These real-world datasets provide valuable opportunities to train our models on diverse, complex scenarios.

Table 1: Summary of datasets and models.

Summary of Datasets				
Name	Scenario	Map	L _I	L _O
Apolloscape [78]	Urban	×	6	6
NGSIM [79]	Highway	×	15	25
nuScenes [80]	Urban	✓	4	12

Trajectory Prediction Model. We used GRIP++ [81] as our prediction model for its proven effectiveness on key trajectory datasets like NGSIM and ApolloScape, which we also employed

Table 2: Summary of GRIP++ model

Name	Input features	Output format	Network
GRIP++ [81]	location + heading	single-prediction	Conv + GRU

in our experiments. GRIP++ consists of three core components: Input Preprocessing, Graph Convolutional Model, and Trajectory Prediction Model with two-layer GRU networks. This design improves predictions for various traffic agents, offering fast, accurate short- and long-term forecasts. GRIP++ runs 21.7 times faster than CS-LSTM and ranked #1 in the ApolloScape competition in 2019, making it an ideal fit for our experiments by minimizing model noise and enhancing algorithm performance evaluation.

5.1 OOD Trajectory Generation

Following [17], we apply random minor perturbation in a single-frame prediction setting for each dataset-model combination. The perturbation alters both spatial coordinates (x-y locations) and features derived from them (e.g., velocity). Further details can be found in §3.3. We assume access to the historical trajectories of all on-road objects when applying perturbations. The average prediction errors before and after perturbation are presented in Table 3. Here, ID denotes in-distribution scenes, while OOD refers to out-of-distribution scenes, where minor perturbations are added to historical trajectories.

Table 3: Average prediction error before and after perturbation

Model	ADE (m)	FDE (m)	RMSE (m)
ApolloScape	1.68 / 4.15	2.11 / 8.73	6.16 / 6.26
NGSIM	4.35 / 7.89	7.50 / 14.82	1.23 / 3.36
nuScenes	5.82 / 8.16	5.03 / 8.78	5.74 / 5.33

5.2 CUSUM Algorithm Applied to Real-world Datasets

To address the challenge of detecting shifts in vehicle behavior from ID to OOD scenarios, we apply the CUSUM algorithm across multiple datasets and metrics, selecting the ApolloScape dataset and ADE for illustration. We observed the sequence $\{x_t\}$ is modeled as Gaussian random variables, with the change assumed to cause a shift in the mean or variance. In the OOD scenario (see Fig. 3a), we observe a significant rise in W_t after the change point, indicating a clear shift in the vehicle’s behavior and reflecting greater uncertainty. In the ID scenario (see Fig. 3b), no change point is detected, as the vehicle’s trajectory remains consistent with typical driving patterns, as illustrated in the upper section of Fig. 1.

The performance of the CUSUM algorithm in detecting uncertainty has proven to be highly accurate in our case. To further enhance its effectiveness, we refined the model by carefully considering the input distribution. Specifically, we observed that the data is better represented by a Gaussian mixture model rather than a simple Gaussian distribution. This insight is based on our knowledge of both the pre-change distribution (f) and post-change distribution (g). As shown in

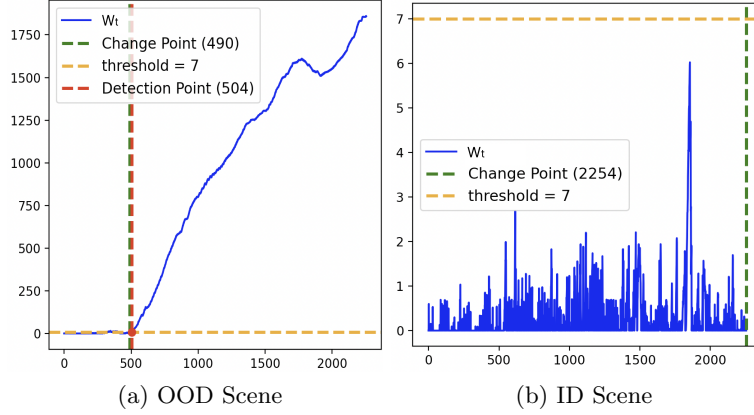


Figure 3: CUSUM Detection (a) OOD Scene. The perturbation is made at time step 490. At time step 507, the statistic W_t exceeds the threshold ($b = 7$), thus the detection of uncertainty is declared. Detection delay is 17.

Fig. 4, the ADE values for both pre-change and post-change distributions of trajectory data from the ApolloScape dataset support this observation. Similar trends and results are consistent across other datasets such as NGSIM and nuScenes, and for additional metrics like FDE and RMSE. Given the page limit constraints, we are not including similar figures in the paper. The performance of the CUSUM algorithm with $\{x_t\}$ modeled using a Gaussian mixture model is reported in the next section.

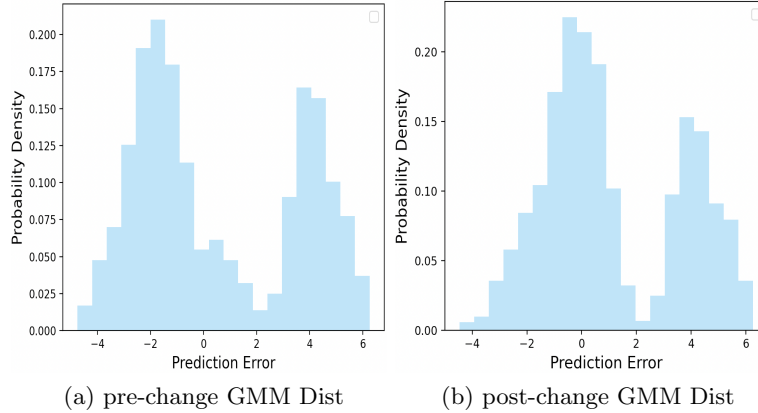


Figure 4: Mix Gaussian Distribution of trajectories from ApolloScape Dataset. ADE metric is applied.

Additionally, we employed the Box-Cox transformation, a well-known parametric technique for reducing anomalies in data [82, 83, 84, 85]. The Box-Cox transformation automatically estimates the optimal λ by maximizing the log-likelihood function, which can be done using statistical software or manually, which in our case, $\lambda = 0.457$. Fig. 5 shows the probability density functions for pre-change and post-change ADE data after the Box-Cox transformer is applied, which the Box-Cox transformation effectively converted the raw data into a near-perfect Gaussian distribution. The performance of the CUSUM algorithm with the Box-Cox transformed data is also reported in the next section.

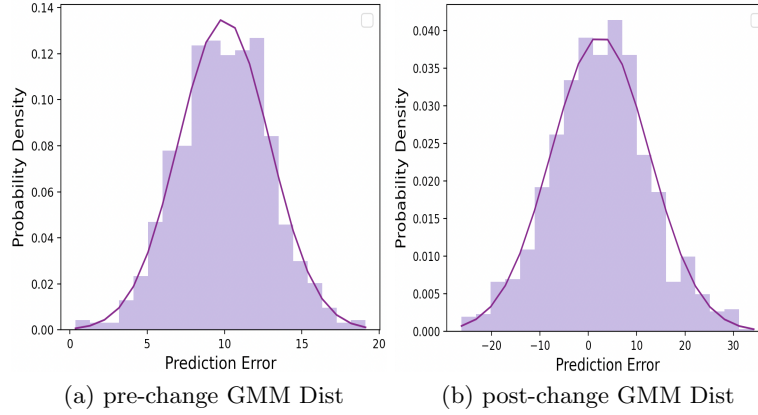


Figure 5: Transformed Gaussian Distribution of trajectories from ApolloScape dataset. ADE metric is applied.

5.3 Evaluation of Detection Performance Across Multiple Algorithms

Our experiments involved 2,254 samples from the ApolloScape dataset, 2,227 samples from NGSIM, and 2,215 samples from nuScenes. All trajectories were predicted using the GRIP++ model, and evaluations were conducted using three metrics: ADE, FDE, and RMSE. We employed standard time-series detection methods, including Z score and chi-square, as benchmarks for detecting possible OOD events in autonomous driving scenarios, and we selected a window size of 50 for moving average calculating of the sequence data. To account for variability in results, we introduced perturbations by randomly selecting change points within a range of approximately 2,000 time steps. This process was repeated iteratively 500 times, and then, we calculate the average detection delay (in time steps) for each algorithm, and the rate of false alarms occurring before the actual change point, which are two standard metrics for evaluation[86]. The detection results are summarized in Table 4.

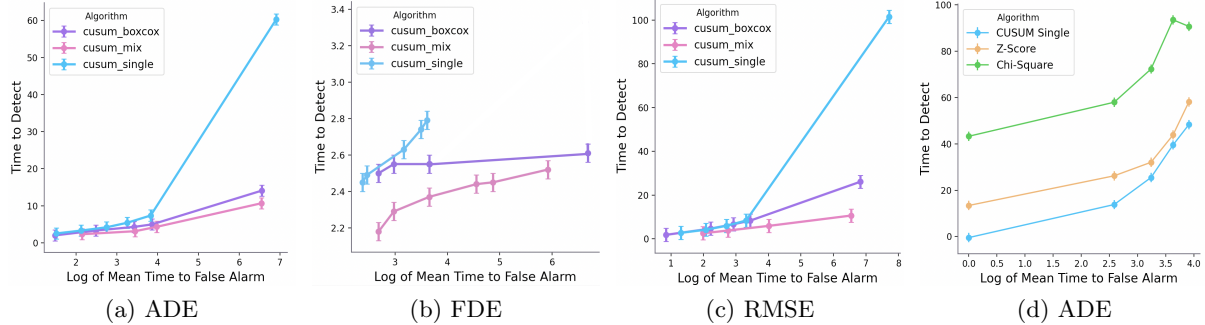


Figure 6: Performance of Delay over Log of Mean Time to False Alarm.

The results indicate that CUSUM algorithms significantly outperform standard time-series methods in detecting OOD events across all datasets. CUSUM Mix achieves the lowest detection delays, with values as low as 0.81 in ApolloScape and 1.25 in NGSIM, while maintaining a low false alarm rate (0.001%–0.025%). CUSUM Transformed follows with moderate detection delays (1.40–2.20) and consistently low false alarm rates (0.000%–0.017%). CUSUM Single, while having the highest detection delays among CUSUM variants (up to 7.50 in NGSIM), still keeps false alarms low (0.000%–0.058%). In contrast, the Z score exhibits much higher delays, reaching 12.2–16.2 in

Table 4: Performance Metrics Comparison Across Datasets

Dataset	Algorithm	Delay			False Alarm Frequency(%)		
		ADE	FDE	RMSE	ADE	FDE	RMSE
ApolloScape	CUSUM Mix	0.81	1.11	1.58	0.025	0.013	0.152
	CUSUM Trans	1.40	2.00	2.70	0.002	0.016	0.037
	CUSUM Single	5.20	2.30	8.70	0.030	0.003	0.000
	Z-Score	12.2	3.00	14.3	0.367	0.410	0.370
	Chi-Square	45.7	68.5	58.1	0.03	0.02	0.04
NGSIM	CUSUM Mix	1.25	1.12	0.90	0.035	0.031	0.032
	CUSUM Trans	2.20	1.30	3.90	0.017	0.000	0.041
	CUSUM Single	7.50	2.10	17.30	0.058	0.000	0.040
	Z-Score	15.5	5.50	27.3	0.359	0.238	0.389
	Chi-Square	68.1	56.6	159.6	0.040	0.010	0.017
nuScenes	CUSUM Mix	0.93	1.06	1.74	0.001	0.241	0.003
	CUSUM Trans	1.70	1.80	2.90	0.000	0.024	0.000
	CUSUM Single	6.50	2.00	7.40	0.019	0.016	0.020
	Z-Score	16.2	3.40	18.7	0.430	0.432	0.428
	Chi-Square	53.1	56.0	60.9	0.011	0.04	0.011

ApolloScape and nuScenes, and has false alarm rates exceeding 35% in several cases. chi-square shows even greater delays, peaking at 68.1 in NGSIM, though with more stable false alarm rates (0.01%–0.04%).

A key observation is that, for the same mean time to a false alarm, better algorithms typically exhibit shorter delays. In our experiment, we first consider normal and OOD scenarios as outlined in Table 3. Assuming no actual change, we measure the time to a false alarm by observing when the algorithm crosses a threshold and triggers a false alarm. To reduce variability, we shuffle the limited number of trajectories 10,000 times, recording the time to false alarm for each shuffle. We follow a similar procedure with OOD data to determine the worst-case delay, then calculate the average time to false alarm and average delay across different thresholds (0.05, 0.1, 0.5, 1, 5, 10, 15).

As shown in Fig. 6 for the ApolloScape dataset, CUSUM Mix consistently has shorter delays than other methods. For instance, at a log mean time to false alarm of 4, CUSUM Mix has an average delay of 4 samples, while CUSUM Single has a delay of 8 samples (Fig. 6a). The CUSUM Transform also outperforms CUSUM Single, as its transformation makes the distribution more Gaussian-like. These trends are consistent across other datasets, though additional figures are not included due to space constraints.

In Fig. 6d, at a mean time to false alarm of 2.5, Z-Score shows 10 more delays than CUSUM Single, while Chi-Square performs even worse, with delays more than 10 times longer. Both algorithms generally show higher ADE, FDE, and RMSE across datasets and metrics.

6 Conclusions

In this paper, we introduced lightweight QCD methods to detect OOD events in real-world trajectory prediction datasets, marking a novel approach in this field. Our approach monitors a scalar variable of prediction errors and handles OOD detection at any point during inference. Our experiments on real-world datasets (ApolloScape, NGSIM, and nuScenes) demonstrated the superiority of CUSUM-based algorithms, particularly when prediction errors were modeled using Gaussian mixture models. CUSUM Mix consistently achieved the lowest detection delays with minimal false alarms, outperforming traditional time-series methods such as Z-Score and Chi-Square. These findings offer a robust solution for enhancing the safety and reliability of AVs through timely model adjustments in dynamic driving environments.

References

- [1] K. Wang, G. Li, J. Chen, Y. Long, T. Chen, L. Chen, and Q. Xia, “The adaptability and challenges of autonomous vehicles to pedestrians in urban china,” *Accident Analysis & Prevention*, vol. 145, p. 105692, 2020.
- [2] S. A. Beiker, “Deployment of automated driving as an example for the san francisco bay area,” in *Road Vehicle Automation 5*. Springer, 2019, pp. 117–129.
- [3] L. Porter, J. Stone, C. Legacy, C. Curtis, J. Harris, E. Fishman, J. Kent, G. Marsden, L. Reardon, and J. Stilgoe, “The autonomous vehicle revolution: Implications for planning/the driverless city?” *Planning Theory & Practice*, vol. 19, no. 5, pp. 753–778, 2018.
- [4] J. Levinson, J. Askeland, J. Becker, J. Dolson, D. Held, S. Kammel, J. Z. Kolter, D. Langer, O. Pink, V. Pratt *et al.*, “Towards fully autonomous driving: Systems and algorithms,” in *2011 IEEE intelligent vehicles symposium (IV)*. IEEE, 2011, pp. 163–168.
- [5] S. Capobianco, L. M. Millefiori, N. Forti, P. Braca, and P. Willett, “Deep learning methods for vessel trajectory prediction based on recurrent neural networks,” *IEEE Transactions on Aerospace and Electronic Systems*, vol. 57, no. 6, pp. 4329–4346, 2021.
- [6] R. Chandra, U. Bhattacharya, A. Bera, and D. Manocha, “Trophic: Trajectory prediction in dense and heterogeneous traffic using weighted interactions,” in *Proceedings of the IEEE/CVF Conference on Computer Vision and Pattern Recognition*, 2019, pp. 8483–8492.
- [7] R. Chandra, T. Guan, S. Panuganti, T. Mittal, U. Bhattacharya, A. Bera, and D. Manocha, “Forecasting trajectory and behavior of road-agents using spectral clustering in graph-lstms,” *IEEE Robotics and Automation Letters*, vol. 5, no. 3, pp. 4882–4890, 2020.
- [8] N. Deo and M. M. Trivedi, “Trajectory forecasts in unknown environments conditioned on grid-based plans,” *arXiv preprint arXiv:2001.00735*, 2020.
- [9] Y. Ma, X. Zhu, S. Zhang, R. Yang, W. Wang, and D. Manocha, “Trafficpredict: Trajectory prediction for heterogeneous traffic-agents,” in *Proceedings of the AAAI conference on artificial intelligence*, vol. 33, no. 01, 2019, pp. 6120–6127.
- [10] Y. Gal *et al.*, “Uncertainty in deep learning,” 2016.
- [11] A. Kendall and Y. Gal, “What uncertainties do we need in bayesian deep learning for computer vision?” *Advances in neural information processing systems*, vol. 30, 2017.
- [12] M. Peng, J. Wang, D. Song, F. Miao, and L. Su, “Privacy-preserving and uncertainty-aware federated trajectory prediction for connected autonomous vehicles,” in *2023 IEEE/RSJ International Conference on Intelligent Robots and Systems (IROS)*. IEEE, 2023, pp. 11 141–11 147.
- [13] H. Huang, S. He, and F. Miao, “Adaptive uncertainty quantification for trajectory prediction under distributional shift,” *arXiv preprint arXiv:2406.12100*, 2024.
- [14] Y. Huang, J. Du, Z. Yang, Z. Zhou, L. Zhang, and H. Chen, “A survey on trajectory-prediction methods for autonomous driving,” *IEEE Transactions on Intelligent Vehicles*, vol. 7, no. 3, pp. 652–674, 2022.

- [15] K. Zhang, L. Zhao, C. Dong, L. Wu, and L. Zheng, “Ai-tp: Attention-based interaction-aware trajectory prediction for autonomous driving,” *IEEE Transactions on Intelligent Vehicles*, vol. 8, no. 1, pp. 73–83, 2022.
- [16] X. Tang, T. Jia, X. Hu, Y. Huang, Z. Deng, and H. Pu, “Naturalistic data-driven predictive energy management for plug-in hybrid electric vehicles,” *IEEE Transactions on Transportation Electrification*, vol. 7, no. 2, pp. 497–508, 2020.
- [17] Q. Zhang, S. Hu, J. Sun, Q. A. Chen, and Z. M. Mao, “On adversarial robustness of trajectory prediction for autonomous vehicles,” in *Proceedings of the IEEE/CVF Conference on Computer Vision and Pattern Recognition*, 2022, pp. 15 159–15 168.
- [18] M. McCloskey and N. J. Cohen, “Catastrophic interference in connectionist networks: The sequential learning problem,” in *Psychology of learning and motivation*. Elsevier, 1989, vol. 24, pp. 109–165.
- [19] Z. Wang, Z. Zhang, C.-Y. Lee, H. Zhang, R. Sun, X. Ren, G. Su, V. Perot, J. Dy, and T. Pfister, “Learning to prompt for continual learning,” in *Proceedings of the IEEE/CVF conference on computer vision and pattern recognition*, 2022, pp. 139–149.
- [20] D. Hendrycks and K. Gimpel, “A baseline for detecting misclassified and out-of-distribution examples in neural networks,” *arXiv preprint arXiv:1610.02136*, 2016.
- [21] K. Lee, H. Lee, K. Lee, and J. Shin, “Training confidence-calibrated classifiers for detecting out-of-distribution samples,” *arXiv preprint arXiv:1711.09325*, 2017.
- [22] K. Lee, K. Lee, H. Lee, and J. Shin, “A simple unified framework for detecting out-of-distribution samples and adversarial attacks,” *Advances in neural information processing systems*, vol. 31, 2018.
- [23] T. Haider, K. Roscher, F. Schmoeller da Roza, and S. Günnemann, “Out-of-distribution detection for reinforcement learning agents with probabilistic dynamics models,” in *Proceedings of the 2023 International Conference on Autonomous Agents and Multiagent Systems*, 2023, pp. 851–859.
- [24] M. H. Danesh and A. Fern, “Out-of-distribution dynamics detection: RL-relevant benchmarks and results,” *arXiv preprint arXiv:2107.04982*, 2021.
- [25] A. Wald, “Sequential tests of statistical hypotheses,” in *Breakthroughs in statistics: Foundations and basic theory*. Springer, 1992, pp. 256–298.
- [26] V. V. Veeravalli and T. Banerjee, “Quickest change detection,” in *Academic press library in signal processing*. Elsevier, 2014, vol. 3, pp. 209–255.
- [27] A. G. Tartakovsky, I. V. Nikiforov, and M. Basseville, *Sequential Analysis: Hypothesis Testing and Change-Point Detection*, ser. Statistics. CRC Press, 2014.
- [28] A. Tartakovsky, *Sequential change detection and hypothesis testing: general non-iid stochastic models and asymptotically optimal rules*. CRC Press, 2019.
- [29] H. V. Poor and O. Hadjiladis, *Quickest detection*. Cambridge University Press, 2009.
- [30] S. Danielsson, L. Petersson, and A. Eidehall, “Monte carlo based threat assessment: Analysis and improvements,” in *2007 IEEE Intelligent Vehicles Symposium*. IEEE, 2007, pp. 233–238.

- [31] D. Bunker, “Classical trajectory methods,“,” *Methods of computational physics*, vol. 10, p. 287, 2012.
- [32] S. Lefèvre, C. Laugier, and J. Ibañez-Guzmán, “Exploiting map information for driver intention estimation at road intersections,” in *2011 IEEE Intelligent Vehicles Symposium (IV)*. IEEE, 2011, pp. 583–588.
- [33] X. Zhang and S. Mahadevan, “Bayesian neural networks for flight trajectory prediction and safety assessment,” *Decision Support Systems*, vol. 131, p. 113246, 2020.
- [34] J. Firl, H. Stübing, S. A. Huss, and C. Stiller, “Predictive maneuver evaluation for enhancement of car-to-x mobility data,” in *2012 IEEE Intelligent Vehicles Symposium*. IEEE, 2012, pp. 558–564.
- [35] N. Ye, Y. Zhang, R. Wang, and R. Malekian, “Vehicle trajectory prediction based on hidden markov model,” 2016.
- [36] J. Li, H. Ma, and M. Tomizuka, “Conditional generative neural system for probabilistic trajectory prediction,” in *2019 IEEE/RSJ International Conference on Intelligent Robots and Systems (IROS)*. IEEE, 2019, pp. 6150–6156.
- [37] F. Altché and A. de La Fortelle, “An lstm network for highway trajectory prediction,” in *2017 IEEE 20th international conference on intelligent transportation systems (ITSC)*. IEEE, 2017, pp. 353–359.
- [38] K. Messaoud, I. Yahiaoui, A. Verroust-Blondet, and F. Nashashibi, “Relational recurrent neural networks for vehicle trajectory prediction,” in *2019 IEEE intelligent transportation systems conference (ITSC)*. IEEE, 2019, pp. 1813–1818.
- [39] N. Deo and M. M. Trivedi, “Multi-modal trajectory prediction of surrounding vehicles with maneuver based lstms,” in *2018 IEEE intelligent vehicles symposium (IV)*. IEEE, 2018, pp. 1179–1184.
- [40] N. Khairdoost, M. Shirpour, M. A. Bauer, and S. S. Beauchemin, “Real-time driver maneuver prediction using lstm,” *IEEE Transactions on Intelligent Vehicles*, vol. 5, no. 4, pp. 714–724, 2020.
- [41] G. Xie, A. Shanguan, R. Fei, W. Ji, W. Ma, and X. Hei, “Motion trajectory prediction based on a cnn-lstm sequential model,” *Science China Information Sciences*, vol. 63, pp. 1–21, 2020.
- [42] H. Woo, Y. Ji, H. Kono, Y. Tamura, Y. Kuroda, T. Sugano, Y. Yamamoto, A. Yamashita, and H. Asama, “Lane-change detection based on vehicle-trajectory prediction,” *IEEE Robotics and Automation Letters*, vol. 2, no. 2, pp. 1109–1116, 2017.
- [43] W. Sun, L. Pan, J. Xu, W. Wan, and Y. Wang, “Automatic driving lane change safety prediction model based on lstm,” in *2024 7th International Conference on Advanced Algorithms and Control Engineering (ICAACE)*. IEEE, 2024, pp. 1138–1142.
- [44] G. Xie, H. Gao, L. Qian, B. Huang, K. Li, and J. Wang, “Vehicle trajectory prediction by integrating physics-and maneuver-based approaches using interactive multiple models,” *IEEE Transactions on Industrial Electronics*, vol. 65, no. 7, pp. 5999–6008, 2017.

- [45] A. Benterki, M. Boukhni, V. Judalet, and C. Maaoui, “Artificial intelligence for vehicle behavior anticipation: Hybrid approach based on maneuver classification and trajectory prediction,” *IEEE Access*, vol. 8, pp. 56 992–57 002, 2020.
- [46] Tishby and Solla, “Consistent inference of probabilities in layered networks: predictions and generalizations,” in *International 1989 joint conference on neural networks*. IEEE, 1989, pp. 403–409.
- [47] D. Feng, A. Harakeh, S. L. Waslander, and K. Dietmayer, “A review and comparative study on probabilistic object detection in autonomous driving,” *IEEE Transactions on Intelligent Transportation Systems*, vol. 23, no. 8, pp. 9961–9980, 2021.
- [48] Y. Gal and Z. Ghahramani, “Dropout as a bayesian approximation: Representing model uncertainty in deep learning,” in *international conference on machine learning*. PMLR, 2016, pp. 1050–1059.
- [49] B. Lakshminarayanan, A. Pritzel, and C. Blundell, “Simple and scalable predictive uncertainty estimation using deep ensembles,” *Advances in neural information processing systems*, vol. 30, 2017.
- [50] M. Bosc, F. Heitz, J.-P. Armspach, I. Namer, D. Gounot, and L. Rumbach, “Automatic change detection in multimodal serial mri: application to multiple sclerosis lesion evolution,” *NeuroImage*, vol. 20, no. 2, pp. 643–656, 2003.
- [51] P. Yang, G. Dumont, and J. M. Ansermino, “Adaptive change detection in heart rate trend monitoring in anesthetized children,” *IEEE transactions on biomedical engineering*, vol. 53, no. 11, pp. 2211–2219, 2006.
- [52] R. Malladi, G. P. Kalamangalam, and B. Aazhang, “Online bayesian change point detection algorithms for segmentation of epileptic activity,” in *2013 Asilomar conference on signals, systems and computers*. IEEE, 2013, pp. 1833–1837.
- [53] T. Lim, A. Soraya, L. Ding, and Z. Morad, “Assessing doctors’ competence: application of cusum technique in monitoring doctors’ performance,” *International Journal for Quality in Health Care*, vol. 14, no. 3, pp. 251–258, 2002.
- [54] J. Reeves, J. Chen, X. L. Wang, R. Lund, and Q. Q. Lu, “A review and comparison of change-point detection techniques for climate data,” *Journal of applied meteorology and climatology*, vol. 46, no. 6, pp. 900–915, 2007.
- [55] N. Itoh and J. Kurths, “Change-point detection of climate time series by nonparametric method,” in *Proceedings of the world congress on engineering and computer science*, vol. 1, 2010, pp. 445–448.
- [56] J.-F. Ducre-Robitaille, L. A. Vincent, and G. Boulet, “Comparison of techniques for detection of discontinuities in temperature series,” *International Journal of Climatology: A Journal of the Royal Meteorological Society*, vol. 23, no. 9, pp. 1087–1101, 2003.
- [57] M. F. R. Chowdhury, S.-A. Selouani, and D. O’Shaughnessy, “Bayesian on-line spectral change point detection: a soft computing approach for on-line asr,” *International Journal of Speech Technology*, vol. 15, pp. 5–23, 2012.

- [58] D. Rybach, C. Gollan, R. Schluter, and H. Ney, "Audio segmentation for speech recognition using segment features," in *2009 IEEE International Conference on Acoustics, Speech and Signal Processing*. IEEE, 2009, pp. 4197–4200.
- [59] R. J. Radke, S. Andra, O. Al-Kofahi, and B. Roysam, "Image change detection algorithms: a systematic survey," *IEEE transactions on image processing*, vol. 14, no. 3, pp. 294–307, 2005.
- [60] A. G. Tartakovsky, A. S. Polunchenko, and G. Sokolov, "Efficient computer network anomaly detection by changepoint detection methods," *IEEE Journal of Selected Topics in Signal Processing*, vol. 7, no. 1, pp. 4–11, 2012.
- [61] A. G. Tartakovsky, B. L. Rozovskii, R. B. Blažek, and H. Kim, "Detection of intrusions in information systems by sequential change-point methods," *Statistical methodology*, vol. 3, no. 3, pp. 252–293, 2006.
- [62] D. R. Jeske, V. M. De Oca, W. Bischoff, and M. Marvasti, "Cusum techniques for timeslot sequences with applications to network surveillance," *Computational statistics & data analysis*, vol. 53, no. 12, pp. 4332–4344, 2009.
- [63] M. Basseville, I. V. Nikiforov *et al.*, *Detection of abrupt changes: theory and application*. prentice Hall Englewood Cliffs, 1993, vol. 104.
- [64] G. Lorden, "Procedures for reacting to a change in distribution," *The annals of mathematical statistics*, pp. 1897–1908, 1971.
- [65] M. Pollak, "Optimal detection of a change in distribution," *The Annals of Statistics*, pp. 206–227, 1985.
- [66] A. N. Shiryaev, *Optimal stopping rules*. Springer Science & Business Media, 2007, vol. 8.
- [67] A. Tartakovsky, "Sequential methods in the theory of information systems," 1991.
- [68] E. S. Page, "Continuous inspection schemes," *Biometrika*, vol. 41, no. 1/2, pp. 100–115, 1954.
- [69] S. Pellegrini, A. Ess, K. Schindler, and L. Van Gool, "You'll never walk alone: Modeling social behavior for multi-target tracking," in *2009 IEEE 12th international conference on computer vision*. IEEE, 2009, pp. 261–268.
- [70] C. Alippi and M. Roveri, "An adaptive cusum-based test for signal change detection," in *2006 IEEE international symposium on circuits and systems*. IEEE, 2006, pp. 4–pp.
- [71] G. Manogaran and D. Lopez, "Spatial cumulative sum algorithm with big data analytics for climate change detection," *Computers & Electrical Engineering*, vol. 65, pp. 207–221, 2018.
- [72] Z. Sun, S. Zou, R. Zhang, and Q. Li, "Quickest change detection in anonymous heterogeneous sensor networks," *IEEE Transactions on Signal Processing*, vol. 70, pp. 1041–1055, 2022.
- [73] C. Cheadle, M. P. Vawter, W. J. Freed, and K. G. Becker, "Analysis of microarray data using z score transformation," *The Journal of molecular diagnostics*, vol. 5, no. 2, pp. 73–81, 2003.
- [74] D. S. Mare, F. Moreira, and R. Rossi, "Nonstationary z-score measures," *European Journal of Operational Research*, vol. 260, no. 1, pp. 348–358, 2017.

- [75] W. A. Wallis and G. H. Moore, “A significance test for time series analysis,” *Journal of the American Statistical Association*, vol. 36, no. 215, pp. 401–409, 1941.
- [76] S. Chiang, J. Zito, V. R. Rao, and M. Vannucci, “Time-series analysis,” in *Statistical Methods in Epilepsy*. Chapman and Hall/CRC, 2024, pp. 166–200.
- [77] T. M. Franke, T. Ho, and C. A. Christie, “The chi-square test: Often used and more often misinterpreted,” *American journal of evaluation*, vol. 33, no. 3, pp. 448–458, 2012.
- [78] X. Huang, X. Cheng, Q. Geng, B. Cao, D. Zhou, P. Wang, Y. Lin, and R. Yang, “The apolloscape dataset for autonomous driving,” in *Proceedings of the IEEE conference on computer vision and pattern recognition workshops*, 2018, pp. 954–960.
- [79] Federal Highway Administration. (2020) Traffic analysis tools: Next generation simulation. [Accessed: Sep. 13, 2024]. [Online]. Available: <https://ops.fhwa.dot.gov/trafficanalysistools/ngsim.htm>
- [80] H. Caesar, V. Bankiti, A. H. Lang, S. Vora, V. E. Liong, Q. Xu, A. Krishnan, Y. Pan, G. Baldan, and O. Beijbom, “nusenes: A multimodal dataset for autonomous driving,” in *Proceedings of the IEEE/CVF conference on computer vision and pattern recognition*, 2020, pp. 11 621–11 631.
- [81] X. Li, X. Ying, and M. C. Chuah, “Grip++: Enhanced graph-based interaction-aware trajectory prediction for autonomous driving,” *arXiv preprint arXiv:1907.07792*, 2019.
- [82] G. E. Box and D. R. Cox, “An analysis of transformations,” *Journal of the Royal Statistical Society Series B: Statistical Methodology*, vol. 26, no. 2, pp. 211–243, 1964.
- [83] R. M. Sakia, “The box-cox transformation technique: a review,” *Journal of the Royal Statistical Society Series D: The Statistician*, vol. 41, no. 2, pp. 169–178, 1992.
- [84] J. Osborne, “Improving your data transformations: Applying the box-cox transformation,” *Practical Assessment, Research, and Evaluation*, vol. 15, no. 1, 2010.
- [85] J. I. Vélez, J. C. Correa, and F. Marmolejo-Ramos, “A new approach to the box-cox transformation,” *Frontiers in Applied Mathematics and Statistics*, vol. 1, p. 12, 2015.
- [86] A. G. Tartakovsky, “Asymptotic optimality in bayesian changepoint detection problems under global false alarm probability constraint,” *Theory of Probability & Its Applications*, vol. 53, no. 3, pp. 443–466, 2009.